



Title	Alternating phase-shifting mask with reduced aberration sensitivity: lithography considerations
Author(s)	Wong, AKK; Liebmann, LW; Molless, AF
Citation	Optical microlithography XIV, Santa Clara, USA, 27 February - 2 March 2001, v. 4346, p. 420-428
Issued Date	2001
URL	http://hdl.handle.net/10722/46226
Rights	Creative Commons: Attribution 3.0 Hong Kong License

Alternating phase-shifting mask with reduced aberration sensitivity: Lithography considerations

Alfred K. Wong^a, Lars W. Liebmann, and Antoinette F. Molless

IBM Semiconductor Research and Development Center
2070 Route 52, Hopewell Junction, NY 12533, USA

^a currently at Department of Electrical and Electronic Engineering
The University of Hong Kong, Pokfulam Road, Hong Kong

ABSTRACT

Aberration sensitivity of alternating phase-shifting masks (PSMs) can be reduced by taking advantage of the trim exposure. Rather than a single phase region bordering each edge of a line, the enhanced alternating PSM technique uses multiple phase regions. The number of phase regions and their widths can be optimized for overall process tolerance including aberration sensitivity and exposure latitude. For exposure with a wavelength of 248 nm and a numerical aperture of 0.68, the optimal number of phase regions is two, with widths between 100 nm and 200 nm. These auxiliary phase regions do not affect the final pattern if a light-field trim mask is used. No extra processing step is necessary. With the enhanced alternating PSM technique, isolated lines of average dimension as small as 36 nm can be delineated using 248 nm lithography with a 3σ linewidth control of 13.4 nm. The mean critical dimension of 36 nm corresponds to $k_1 = 0.1$.

Keywords: optical lithography, phase-shifting mask, aberrations, alternating phase-shifting mask, enhanced alternating phase-shifting mask

1. INTRODUCTION

Alternating phase-shifting masks (PSMs)¹ offer robust imaging of small, dark regions. Field-effect transistors (FETs) with gate lengths corresponding to $k_1 = 0.2$ ² and isolated linewidths of $k_1 = 0.1$ ³ have been demonstrated. Superior aerial image quality and lower sensitivity to mask critical dimension (CD) error⁴ of alternating PSMs compared with chromium-on-glass (COG) masks hold the promise of reduced across-chip linewidth variation (ACLV). Nevertheless, implementation of alternating PSMs is not straightforward. Issues include intensity imbalance due to mask topography,⁵⁻⁷ mask inspection and repair,⁸⁻¹⁰ and the need for sophisticated computer-aided design (CAD) algorithms.¹¹ The existence of more than one phase on the photomask means that aberration sensitivity is also a concern. This work aims to examine aberration sensitivity of alternating PSMs, and possible approaches for its reduction.

2. ALTERNATING PSM AND COG MASK

Let us first compare the simulated aberration sensitivity of an isolated line printed with a COG mask and an alternating PSM, as shown in Fig. 1. The 100-nm line is imaged with an exposure system with a wavelength of 248 nm ($\lambda = 248$ nm), a numerical aperture of 0.68 ($NA = 0.68$), and a partial coherence factor of 0.3 ($\sigma = 0.3$). With these parameters, the 100-nm line corresponds to $k_1 = 0.27$. Aberration sensitivity is determined for each Zernike polynomial Z_i ,¹² being measured by the difference between the aerial image with no aberrations, except for a focus error of 250 nm,* and the image with 0.01λ of

E-mail: A. K. W.—awong@eee.hku.hk; L. W. L.—lliebman@us.ibm.com; A. F. M.—amolless@us.ibm.com

*A 250-nm focus error is approximately 1 R. U., where R. U. is the Rayleigh unit of depth of focus ($\frac{\lambda}{2NA^2}$).

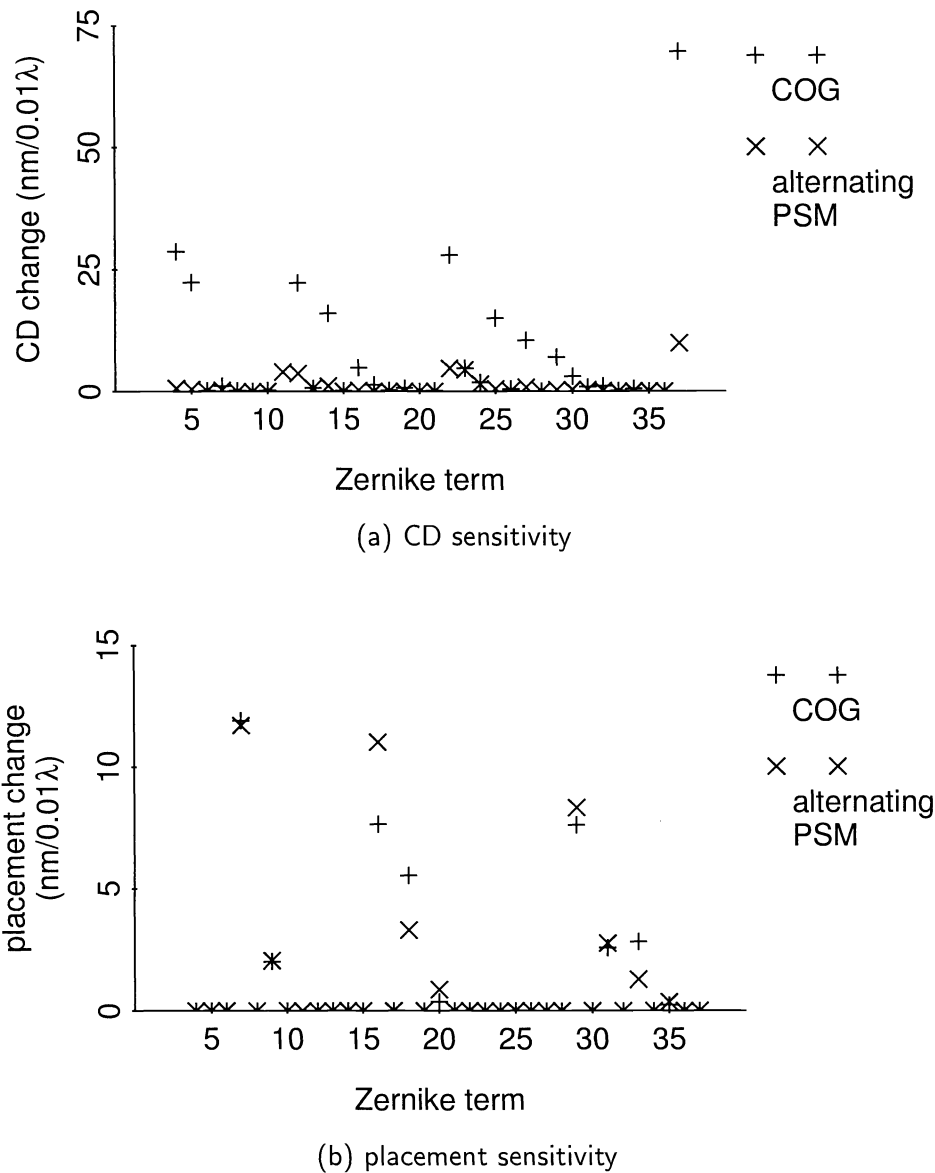


Figure 1. Aberration sensitivity of a $k_1 = 0.27$ line. The Zernike terms are tabulated in Appendix A.

Z_i with the same focus error.^{13,14} For sensitivity of the critical dimension to aberrations, as shown in Fig. 1(a), an alternating PSM is consistently better than a COG mask, a phenomenon also observed by other authors.^{15,13} This result is a consequence of the better quality of the alternating PSM image.

For placement sensitivity to aberrations, however, an alternating PSM does not have much advantage over a COG mask. Both types of mask are similarly sensitive to the various orders of coma (terms 7, 16, and 29) and three-leaf clover (terms 9, 18, and 31), as shown in Fig. 1(b). For 0.01λ of third order coma aberration, the 100-nm isolated line is shifted by 12 nm, amounting to 12% of the CD.

Aberration sensitivity of an alternating PSM can be decreased by exposure with a larger partial coherence factor. As shown in Fig. 2(a), the placement sensitivity is decreased by large factors when the partial coherence factor increases from 0.3 to 0.7. For example, placement sensitivity to third order coma reduces from 12 nm to 4.7 nm for a 100-nm isolated line. However, increasing the partial coherence factor has the unfortunate effect of exposure latitude and depth of focus reduction [Fig. 2(b)]. As σ increases from 0.3 to

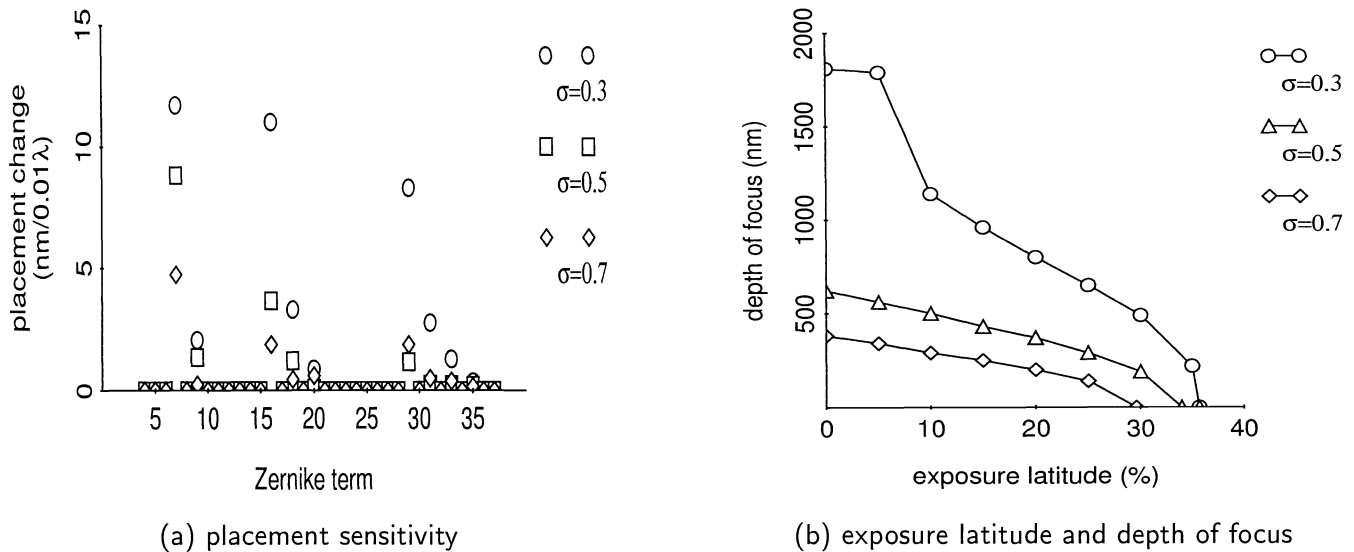


Figure 2. Aberration sensitivity improves with increasing partial coherence factor, while both exposure latitude and depth of focus decreases.

0.5, the total window¹⁶ decreases from 34.4 % μm to 13.1 % μm .[†] A further increase of the partial coherence factor to 0.7 almost halves the total window to 7.0 % μm . It is desirable to reduce aberration sensitivity of alternating PSMs without the significant reduction in depth of focus and exposure latitude.

3. THROUGH-PITCH ABERRATION SENSITIVITY

We can obtain clues for aberration sensitivity reduction by observing the dependence of aberration sensitivity on pitch. Figure 3(a) shows the placement sensitivity of a 100-nm line to third order coma aberration as a function of pitch. For periods larger than 400 nm, the sensitivity is fairly constant at 12 nm/0.01λ. But it drops rapidly below a pitch of 400 nm, reaching a value as low as 2 nm/0.01λ for a period of 250 nm before increasing at smaller pitches. This increase originates from poor image quality, rather than high aberration sensitivity per se—a 200-nm period is very close to the theoretical resolution limit of the exposure system of 182 nm. We can therefore assert that aberration sensitivity decreases with decreasing pitch, until the period is so small that even the image with no aberrations is not useful. On the other hand, the exposure latitude of the 100-nm line is relatively stable as a function of pitch (except for very small periods where image quality is poor). As shown in Fig. 3(b), the exposure latitude for pitch values greater than 250 nm is approximately 35%. From exposure latitude and aberration sensitivity considerations, we would like to print patterns with periods around 250 nm.

4. ENHANCED ALTERNATING PSM

For the exposure system under consideration, a pitch of 250 nm results in low aberration sensitivity and uncompromised exposure latitude. From the lithography point of view, it is thus advantageous to introduce forbidden pitches such that patterns with periods greater than, say, 300 nm are not allowed. Such design rules are usually excessively restrictive on circuit design. By using light-field trim masks and dark-field alternating PSMs with certain modifications, it is possible to print lines with reduced aberration sensitivity, without much sacrifice in exposure latitude, and with less severe design restrictions. Let us illustrate the

[†]The total window numbers are the areas enclosed by the depth-of-focus-exposure-latitude curves and the axes [Fig. 2(b)].

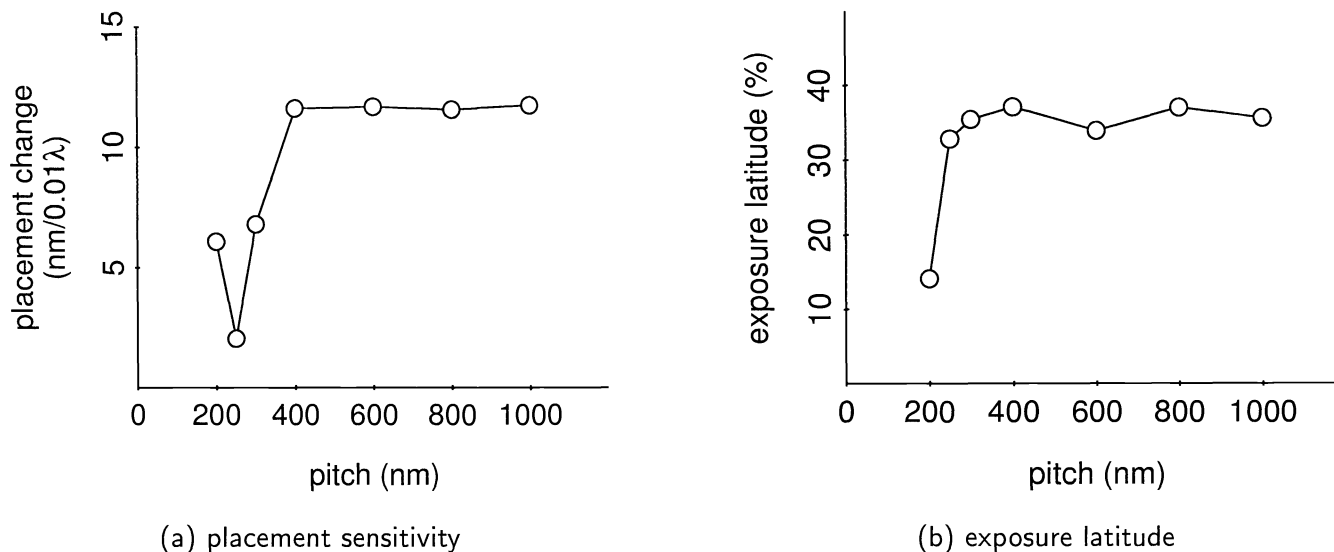


Figure 3. Dependence of process tolerance on pitch.

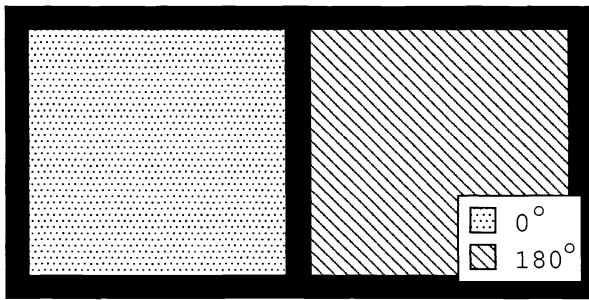
method by Fig. 4. In the traditional approach, a line is formed by combining the images of the alternating PSM [Fig. 4(a)] and the trim mask [Fig. 4(b)]. Conventional wisdom says that the width of the phase regions on the alternating PSM should be made large, since the exposure latitude increases with increasing phase width, as shown in Fig. 5(a). But increasing the phase width also increases aberration sensitivity, as shown in Fig. 5(b). To balance the competing requirements of low dose sensitivity and low aberration sensitivity, we propose forming a line by adding the images of an alternating PSM with multiple phase regions [Fig. 4(c)] and a light-field trim mask [Fig. 4(b)]. This method has the advantage of allowing us to adjust the number of phase regions and their widths to optimize for overall process tolerance including aberration sensitivity and exposure latitude.

The optimization problem is similar to that of placing assist features¹⁷ and phase-shifting assist features.¹⁸ Rather than adding assist features which are the same tone as the main pattern, however, we place features that are of the opposite tone. Moreover, we do not worry if these auxiliary phase regions print, because any trace of their existence is removed by the light-field trim mask.

To simplify the optimization, we investigate the situation where the widths of the phase areas [the dimension s in Fig. 4(c)] are uniform, and the opaque lines separating the phase regions have the same dimension as the main feature [$w = CD$ in Fig. 4(c)]. The problem becomes determining the number of phase regions on each side of the line (n) and their sizes s . The curve with the circular markers in Fig. 6 shows the aberration sensitivity of an isolated 100-nm line bordered by one phase region ($n = 1$) as a function of the phase width (s). The sensitivity to third order coma decreases with reducing phase width, a result that is consistent with the data shown in Fig 3(a). For minimal aberration sensitivity, we would like to have as narrow a phase width as possible,[‡] and the maximum phase width should be around 200 nm.

The phase width cannot be arbitrarily small. The minimum phase width is constraint on the one hand by mask-making limitations, and on the other hand by the need to maintain adequate image quality. For an exposure system with a 2% flare, the dose sensitivity as a function of phase width is shown by the curve with the square markers in Fig. 6. The dose sensitivity shown is the CD change with a 10% dose variation. As the phase width decreases from 300 nm, the dose sensitivity starts to increase. To maintain adequate

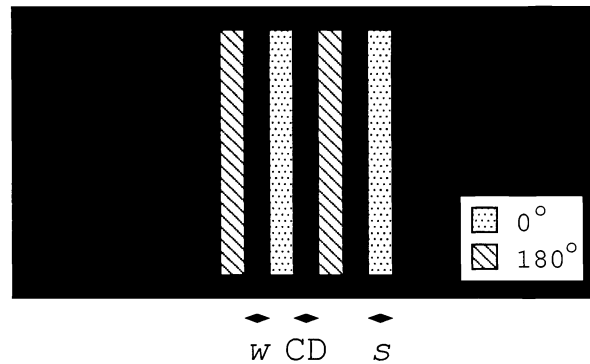
[‡]In the limit of $s = 0$, there is no aberration sensitivity because we have no image anymore.



(a) traditional alternating PSM

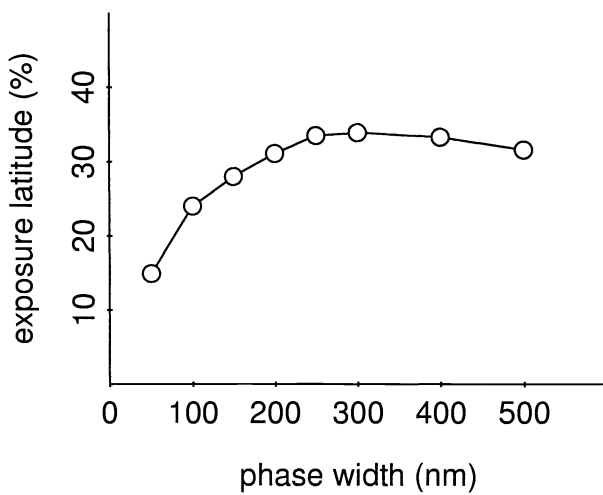


(b) light-field trim

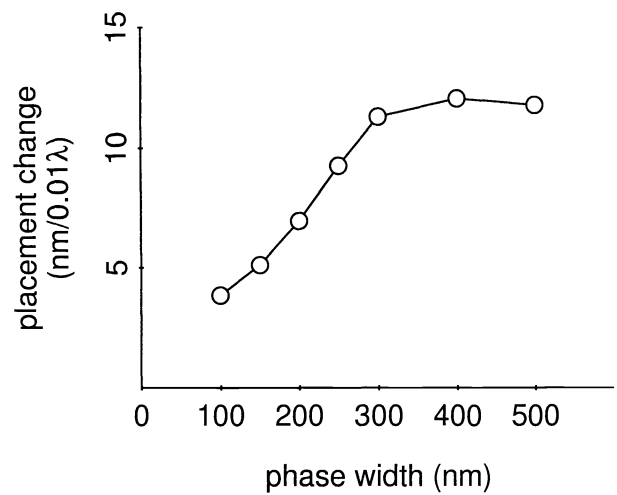


(c) enhanced alternating PSM

Figure 4. A line can be formed by combining the light-field trim mask (b) with either the traditional alternating PSM (a) or the enhanced alternating PSM (c).



(a) exposure latitude



(b) placement sensitivity

Figure 5. Both aberration sensitivity and exposure latitude decrease as a function of phase width.

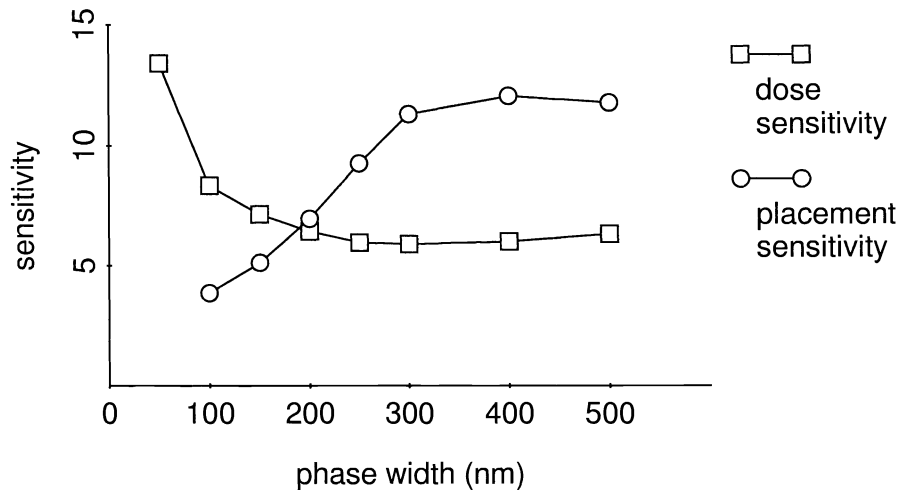


Figure 6. A balance can be maintained between dose and aberration sensitivities.

latitude, the minimum phase width should be approximately 100 nm. Together with the upper-bound determined from aberration sensitivity considerations, the phase width should range from 100–200 nm.

With the bounds of the phase width defined, we need to determine the optimal number of phase regions (n). Figure 7 shows the placement sensitivity of a 100-nm line to third order coma aberration as a function of the number of phase regions, whose widths are 100 nm. There is a reduction in aberration sensitivity as n increases from 1 to 2. But subsequent increase in n causes the sensitivity to increase. This phenomenon arises because the additional phase regions effectively transform the original isolated line into a periodic pattern with a 200-nm pitch, whose aberration sensitivity is high because of poor image quality [Fig. 3(a)]. If we set the phase width to 150 nm, the aberration sensitivity converges to a low value with increasing n , as shown in Fig. 8. The asymptotic value of $2.2 \text{ nm}/0.01\lambda$ is reached when n is as small as 2 ($n = 2$). Since two phase regions are adequate, the width of the regions (s) can be as small as 100 nm without worries of increased aberration sensitivity with larger values of n [Fig. 7].

Summarizing the above results, a balance between aberration and dose sensitivity can be achieved by using extra phase regions on an alternating PSM. For the exposure system under consideration ($\lambda = 248 \text{ nm}$, $NA = 0.68$), the minimum phase width is 100 nm and the number of phase regions per line edge is two. We call this technique of adding extra phase regions for aberration sensitivity reduction “enhanced alternating PSM.”[§]

5. EXPERIMENTAL RESULTS

Experimentally measured linewidth variation as a function of the average CD is plotted in Fig. 9. The isolated line was designed using an enhanced alternating PSM with a CD of 125 nm and 2 phase regions whose widths (s) are 125 nm. The various mean CDs were achieved by exposure dose changes. Linewidth variation is expressed in 3σ numbers; each datum in the figure was calculated from analysis of 4,000 electrical linewidth measurement data using the spatial dissection method.¹⁹ Isolated lines with an average dimension of 36 nm were printed with a 3σ variation of 13.4 nm. This critical dimension corresponds to $k_1 = 0.1$.

[§]This nomenclature is due to Juergen Preuninger at Infineon.

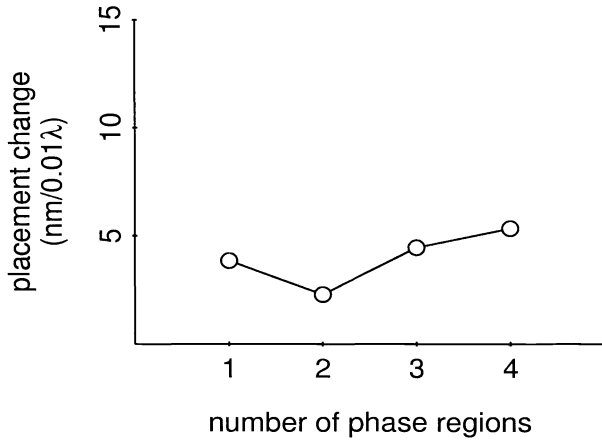


Figure 7. Placement sensitivity of a 100-nm isolated line with different numbers of 100-nm phase regions.

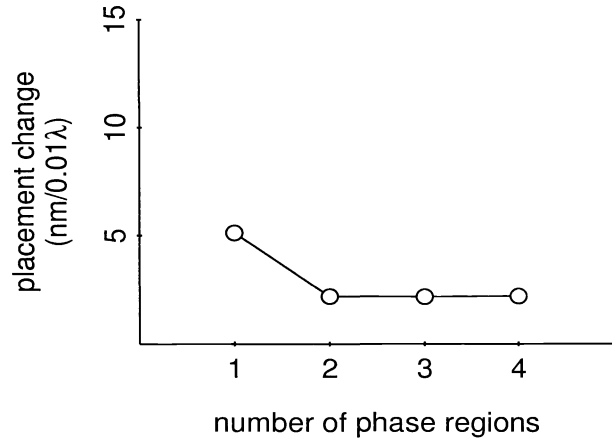


Figure 8. Placement sensitivity of a 100-nm isolated line with different numbers of 150-nm phase regions.

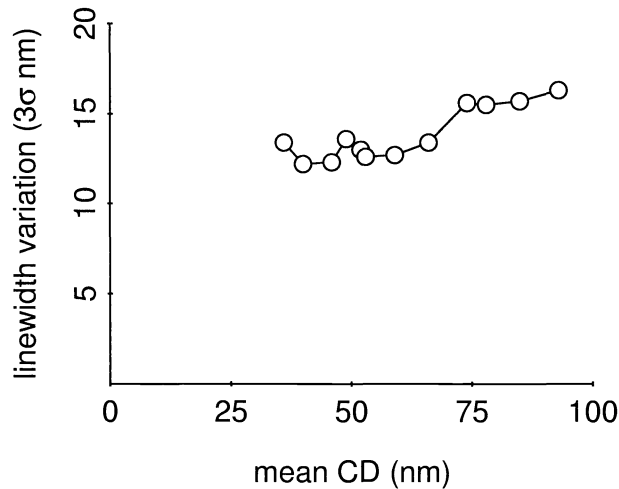


Figure 9. Experimentally measured linewidth variation as a function of nominal CD. Isolated lines as small as 36 nm were printed with good dimension control using enhanced alternating PSM.

6. DISCUSSION

By using extra phase regions on an alternating PSM to decrease the effective pattern period, aberration sensitivity is reduced. This technique is applicable to processes using dark-field alternating PSMs and light-field trim masks. Since dark-field alternating PSM is preferred because of mask inspection and defect issues, the use of enhanced alternating PSM does not result in additional processing steps. It is entirely consistent with the existing technology. Lines as small as 36 nm ($k_1 = 0.1$) were demonstrated with a linewidth control of 13.4 nm (3σ).

The use of multiple phase regions creates a design problem similar to that of assist feature optimization. The placement and sizing of the auxiliary phase regions require software whose intelligence is no less than those of phase assignment algorithms.²⁰⁻²³ In order to maintain a low overall aberration sensitivity, forbidden pitches may need to be introduced. But the improved lithography performance of enhanced alternating PSM is well worth these added complexities.

APPENDIX A. LIST OF ZERNIKE POLYNOMIALS

Ordering of the Zernike polynomials in the figures is similar to that by Mahajan.¹²

Term	$Z_j(\rho, \phi)$
1	$\sqrt{1}$ (+1)
2	$\sqrt{4}$ $(+\rho)\cos \phi$
3	$\sqrt{4}$ $(+\rho)\sin \phi$
4	$\sqrt{3}$ $(+2\rho^2 - 1)$
5	$\sqrt{6}$ $(+\rho^2)\cos 2\phi$
6	$\sqrt{6}$ $(+\rho^2)\sin 2\phi$
7	$\sqrt{8}$ $(+3\rho^3 - 2\rho)\cos \phi$
8	$\sqrt{8}$ $(+3\rho^3 - 2\rho)\sin \phi$
9	$\sqrt{8}$ $(+\rho^3)\cos 3\phi$
10	$\sqrt{8}$ $(+\rho^3)\sin 3\phi$
11	$\sqrt{5}$ $(+6\rho^4 - 6\rho^2 + 1)$
12	$\sqrt{10}$ $(+4\rho^4 - 3\rho^2)\cos 2\phi$
13	$\sqrt{10}$ $(+4\rho^4 - 3\rho^2)\sin 2\phi$
14	$\sqrt{10}$ $(+\rho^4)\cos 4\phi$
15	$\sqrt{10}$ $(+\rho^4)\sin 4\phi$
16	$\sqrt{12}$ $(+10\rho^5 - 12\rho^3 + 3\rho)\cos \phi$
17	$\sqrt{12}$ $(+10\rho^5 - 12\rho^3 + 3\rho)\sin \phi$
18	$\sqrt{12}$ $(+5\rho^5 - 4\rho^3)\cos 3\phi$
19	$\sqrt{12}$ $(+5\rho^5 - 4\rho^3)\sin 3\phi$
20	$\sqrt{12}$ $(+\rho^5)\cos 5\phi$
21	$\sqrt{12}$ $(+\rho^5)\sin 5\phi$
22	$\sqrt{7}$ $(+20\rho^6 - 30\rho^4 + 12\rho^2 - 1)$
23	$\sqrt{14}$ $(+15\rho^6 - 20\rho^4 + 6\rho^2)\cos 2\phi$
24	$\sqrt{14}$ $(+15\rho^6 - 20\rho^4 + 6\rho^2)\sin 2\phi$
25	$\sqrt{14}$ $(+6\rho^6 - 5\rho^4)\cos 4\phi$
26	$\sqrt{14}$ $(+6\rho^6 - 5\rho^4)\sin 4\phi$
27	$\sqrt{14}$ $(+\rho^6)\cos 6\phi$
28	$\sqrt{14}$ $(+\rho^6)\sin 6\phi$
29	$\sqrt{16}$ $(+35\rho^7 - 60\rho^5 + 30\rho^3 - 4\rho)\cos \phi$
30	$\sqrt{16}$ $(+35\rho^7 - 60\rho^5 + 30\rho^3 - 4\rho)\sin \phi$
31	$\sqrt{16}$ $(+21\rho^7 - 30\rho^5 + 10\rho^3)\cos 3\phi$
32	$\sqrt{16}$ $(+21\rho^7 - 30\rho^5 + 10\rho^3)\sin 3\phi$
33	$\sqrt{16}$ $(+7\rho^7 - 6\rho^5)\cos 5\phi$
34	$\sqrt{16}$ $(+7\rho^7 - 6\rho^5)\sin 5\phi$
35	$\sqrt{16}$ $(+\rho^7)\cos 7\phi$
36	$\sqrt{16}$ $(+\rho^7)\sin 7\phi$
37	$\sqrt{9}$ $(+70\rho^8 - 140\rho^6 + 90\rho^4 - 20\rho^2 + 1)$

ACKNOWLEDGMENTS

The authors are grateful for input from Scott Bukofsky, Tim Farrell, Gerard Kunkel, Juergen Preuninger, and Alan Thomas.

REFERENCES

1. M. Levenson, N. Viswanathan, and R. Simpson, "Improving resolution in photolithography with a phase-shifting mask," *IEEE Transactions on Electron Devices* **29**, pp. 1812–1846, Dec. 1982.
2. T. Brunner, P. Sanda, M. Wordeman, and T. Lii, "170 nm gates fabricated by phase-shift mask and top anti-reflector process," in *Proc. SPIE*, J. Cuthbert, ed., vol. 1927, pp. 182–189, 1993.
3. S. Nakao, J. Itoh, A. Nakae, I. Kanai, T. Saitoh, H. Matsubara, K. Tsujita, I. Arimoto, and W. Wakamiya, "Extension of KrF lithography to sub-50 nm pattern formation," in *Proc. SPIE*, C. Proglor, ed., vol. 4000, pp. 358–365, 2000.
4. A. Wong, R. Ferguson, and S. Mansfield, "The mask error factor in optical lithography," *IEEE Transactions on Semiconductor Manufacturing* **13**, pp. 235–242, May 2000.
5. R. Kostelak, C. Pierrat, J. Garofalo, and S. Vaidya, "Exposure characteristics of alternate aperture phase-shifting masks fabricated using a subtractive process," *J. Vac. Sci. Technol. B* **10**, pp. 3055–3061, Nov. 1992.
6. A. Wong and A. Neureuther, "Mask topography effects in projection printing of phase-shifting masks," *IEEE Transactions on Electron Devices* **41**, pp. 895–902, June 1994.
7. R. Ferguson, L. Liebmann, S. Mansfield, D. O'Grady, and A. Wong, "Exact transmission balanced alternating phase-shifting mask for photolithography." U.S. patent #5932377, Aug. 1999.
8. J. N. Wiley, T. Y. Fu, T. Tanaka, S. Takeuchi, S. Aoyama, J. Miyazaki, and Y. Watakabe, "Phase shift mask pattern accuracy requirements and inspection technology," in *Proc. SPIE*, W. H. Arnold, ed., vol. 1464, pp. 346–355, SPIE, 1991.
9. L. Liebmann, S. Mansfield, A. Wong, J. Smolinski, S. Peng, K. Kimmel, M. Rudzinski, J. Wiley, and L. Zurbrick, "High-resolution ultraviolet defect inspection of DAP (darkfield alternate phase) reticles," in *Proc. SPIE*, F. Abboud and B. Grenon, eds., vol. 3873, pp. 148–161, 1999.
10. A. K. Wong, *Resolution Enhancement Techniques in Optical Lithography*, section 5.3.3, pp. 128–130. SPIE Press, 2001.
11. L. Liebmann, S. Mansfield, A. Wong, M. Lavin, W. Leipold, and T. Dunham, "TCAD/EDA development for lithography resolution enhancement," *IBM J. Res. Develop.*, 2001.
12. V. N. Mahajan, "Zernike circle polynomials and optical aberrations of systems with circular pupils," *Engineering & Laboratory Notes*, pp. S-21–S-24, Aug. 1994.
13. R. Schenker, "Effects of phase shift masks on across field linewidth control," in *Proc. SPIE*, L. van den Hove, ed., vol. 3679, pp. 18–26, 1999.
14. C. Proglor and A. Wong, "Zernike coefficients: are they really enough?," in *Proc. SPIE*, C. Proglor, ed., vol. 4000, pp. 40–52, 2000.
15. H.-Y. Liu, L. Karklin, Y.-T. Wang, and Y. C. Pati, "The application of alternating phase-shifting masks to 140 nm gate patterning: Line width control improvements and design optimization," in *Proc. SPIE*, vol. 3236, pp. 328–337, 1998.
16. A. Wong, R. Ferguson, S. Mansfield, A. Molless, D. Samuels, R. Schuster, and A. Thomas, "Level-specific lithography optimization for 1 Gb DRAM," *IEEE Transactions on Semiconductor Manufacturing* **13**, pp. 76–87, Feb. 2000.
17. S. M. Mansfield, L. W. Liebmann, A. F. Molless, and A. K. Wong, "Lithographic comparison of assist feature design strategies," in *Proc. SPIE*, C. Proglor, ed., vol. 4000, pp. 63–76, 2000.
18. M. D. Prouty and A. R. Neureuther, "Optical imaging with phase shift masks," in *Proc. SPIE*, vol. 470, pp. 228–232, 1984.
19. A. K. Wong, A. F. Molless, T. A. Brunner, E. Coker, R. H. Fair, G. L. Mack, and S. M. Mansfield, "Characterization of line width variation," in *Proc. SPIE*, C. Proglor, ed., vol. 4000, pp. 184–191, 2000.
20. Y. C. Pati and T. Kailath, "Phase-shifting masks for microlithography: automated design and mask requirements," *J. Opt. Soc. Am. A* **11**, pp. 2438–2452, Sept. 1994.
21. K. Ooi, K. Koyama, and M. Kiryu, "Method of designing phase-shifting masks utilizing a compactor," *Jpn. J. Appl. Phys.* **33**, pp. 6774–6778, Dec. 1994.
22. A. Moniwa, T. Terasawa, K. Nakajo, J. Sakemi, and S. Okazaki, "Heuristic method for phase-conflict minimization in automatic phase-shift mask design," *Jpn. J. Appl. Phys.* **34**, pp. 6584–6589, Dec. 1995.
23. T. Haruki, R. Tsujimura, J. Tomida, Y. Machida, S. Asai, and I. Hanju, "Development of total support CAD system for alternate-type PSMs with optical proximity correction," in *Proc. SPIE*, vol. 3748, pp. 222–232, 1999.